Chapter 13

Crystallization of Fe and Mn Oxides-Hydroxides in Saline and Hypersaline Enviro nments and In vitro

Nurit Taitel-Goldman

Additional information is available at the end of the chapter

http://dx.doi.org/10.5772/59625

1. Introduction

Iron oxides crystallize in various enviro nments. This chapter focuses on short-range ordered or well-crystallized iron oxides and Fe - Mn oxides that crystallize in saline and in hypersaline enviro nments or in similar conditions in vitro.

1.1. Geological background

In the actively diverging central part of the Red Sea, a series of submarine Deeps were formed (Figure 1a). Red Sea deep water interacts with hot magmatic rocks, dissolves salt layers and then discharges into the Deeps creating hydrothermal hypersaline brine that feeds the Deeps. A hydrothermal hypersaline brine (68°C, 270‰) [1] discharges into the southwestern basin of Atlantis II Deep located between 21°19N and 21°27N and is 15 km long and 8 km wide (Figure 1b). The water depth reaches 2190 m. [2, 3, 4]. The hydrothermal hypersaline brine forms a stable stratified water column resulting from density differences. Iron concentration increases with depth from 0.01 m g/kg to 75-81 m g/kg in the lower brine. Mn concentration in the lower brine is 82 m g/kg whereas in the Red Sea deep water, it is 0.009 m g/kg [5]. Mixing between the discharging brine and the aerobic Red Sea deep water, which occurs at the depth of 2008-1990m below sea level, leads to iron oxidation and crystallization of iron oxide-hydroxides. Variability in iron oxides or hydroxides results from the conditions in which they crystallized.

The hypersaline and hydrothermal brine that fills the Atlantis II Deep overflows into the close Chain and Discovery Deeps. This leads to elevated temperatures in the lower water layer in the Discovery Deep that reach 48°C. Lately it was suggested that hydrothermal brine also discharges into the Discovery Deep which has lead to a constant temperature over the last 40 years [1] The elevated temperature salinity and iron concentrations lead to crystalliza-

tion of iron and manganese oxides or hydroxides in these Deeps as well. Mn-Fe oxide-hydroxides were crystallized either in the margins of the Deeps or close to the interface between the hydrothermal brines and the overlying aerobic Red Sea deep water. Fe-oxides that crystallize in the oxic-unoxic boundary settle down to the Deep floor whereas Mn oxides-hydroxides dissolve while settling down on the Deep floor but they accumulate on the flanks of the Deeps [6].

Iron oxides were collected from sediments of the Thetis Deep in the Red Sea located between 22°46N and 22°49N with a water depth of 1780m (Figure 1c). Currently, no hydrothermal brine discharges into this Deep, yet it is possible that hydrothermal brine was present in the Thetis Deep during deposition of iron oxides [7]. Cores studied from the Thetis Deep have a higher Fe and Mn oxide-hydroxides than cores sampled outside the Deep. Similarly, V, Cu, Zn, and Pb are enriched in Thetis Deep sediments [8].

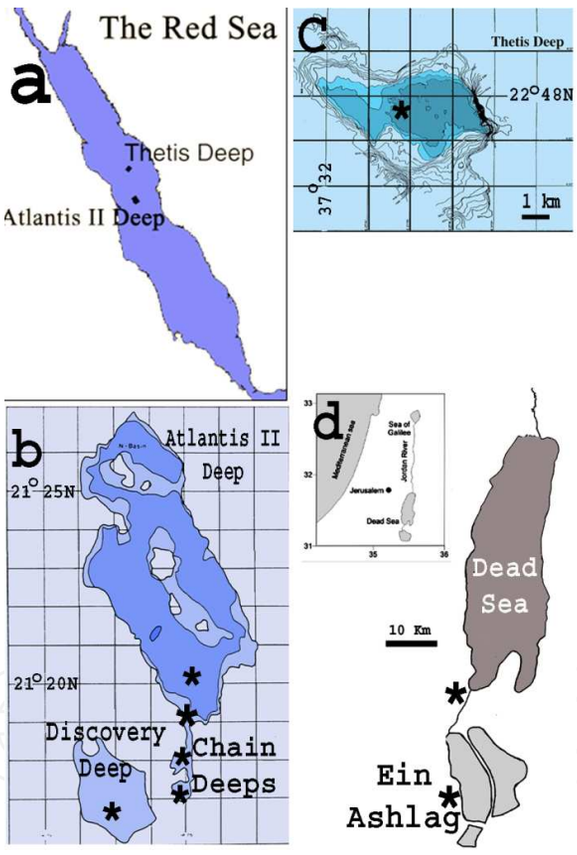

Figure 1. Location maps: a) Red Sea; b) Atlantis II Deep, Chain Deeps and Discovery Deep; c) Thetis Deep; d) Dead Sea area and in the upper part of the map of Israel with the Dead Sea location. Ein-Ashlag seepage is in the southern part of the dead Sea on the eastern flank of the Mount Sedom diapir. (*- sampling area)

Dead Sea samples were collected near saline springs that discharge close to the Dead Sea or from Ein-Ashlag located on the eastern flanks of Mount Sedom diapir (Figure 1d). The springs and Dead Sea water are Ca-Chloride hypersaline brine, initially formed in a Pliocene lagoon. The salinity of the Dead Sea reaches 340 g/l [9]. Ein-Ashlag is a hypersaline seepage that results

http://dx.doi.org/10.5772/59625

from hypersaline brine body that is associated with Mt. Sedom salt diapir. The salinity of the seepage (390 TDS/l) is even higher than Dead Sea water (340gTDS/l). The amount of dissolved Fe^{2+} in the Ein-Ashlag spring is 0.12 g/l [10] Initially formed iron and manganese oxides that crystallize close to the discharging spring are commonly preserved within halite crystals, hence their initial composition remains and recrystallization processes are restrained.

Minerals presented in this chapter are short-range ordered ferrihydrite ($Fe_5HO_8*4H_2O$), singerite ($SiFe_4(OH)_4*H_2O$) and Mn-oxide-hydroxide layers. Well- crystallized phases presented are goethite ((αFeOOH), akaganéite (βFeOOH), lepidocrocite (γFeOOH), feroxyhyte (δFeOOH), hematite (αFe_2O_3), magnetite (Fe_3O_4), todorokite ($(Ca, mg)_{1-x}Mn^{4+}O_{12}$ *3-4 H_2O), groutite (αMnOOH) and manganite (γMnOOH). Laboratory imitation of the hydrothermal and hypersaline enviro nments enabled the understanding of the conditions in which each phase precipitated.

2. Methods

Morphology of the phases was observed using high resolution scanning electron microscopy (HRSEM) or high resolution transmission electron microscopy (HRTEM). Using point analyses, a solid solution between two phases or impurities within crystals were detected. In most of the samples studied, the fine fraction was checked with High Resolution Transmission Electron Microscopy using a JEOL FasTEM 2010 electron microscope equipped with a Noran energy dispersive spectrometer (EDS) for microprobe elemental analyses. The results presented are in atomic ratios. Beam width for point analyses was 25 nm. Crystalline phases or short-range ordered phases were identified using selected area electron diffraction (SAED) in the HRTEM. The smallest area for SAED was 100 nm. The data obtained from the HRTEM were processed using fast Fourier transformation with Digital Micrograph (Gatan) software.

3. Short-range ordered phases

3.1. Crystallization of short-range ordered ferrihydrite in the Red Sea and in the Dead Sea area

Nanometer-size phases showing short range periodity are common in the newly formed sediments in the hydrothermal hypersaline enviro nment of the Red Sea and in the Dead Sea area. Ferrihydrite (<10 nm) has euhedral to subhedral morphology and a short-range ordered pattern in the inner part. Crystallization of ferrihydrite occurs as dissolved Fe oxidizes at the presence of dissolve Si that hinders crystal growth so nano-sized crystals are formed with Si impurity with Si/Fe molar ratios varying between 0.17-0.89.

The initial stage of ferrihydrite formation was observed on a plastic bag floating in the Dead Sea water close to a discharging spring with a Si/Fe atomic ratio of 0.26 (Figure 2a). Other ferrihydrite crystals in the Dead Sea were preserved within halite crystals that prevented

recrystallization processes. Point analyses in ferrihydrite crystals yielded Si and Mn impurities with ratios of Si/Fe 0.105 and Mn/Fe 0.013 (Figure 2b).

2-line ferrihydrite clusters of 200 nm were found in samples from the uppermost layer of sediments in the Atlantis II Deep at a water depth of 2165m, [11]. The ferrihydrite presented (Figure 2c) was suspended in the lowermost 10 cm of the hydrothermal brine with a crystal size of 5 nm and point analyses yielded a Si/Fe elevated 0.53 ratio (Figure 2c).

Mn and Fe share similar atomic size (0.645 nm), hence formation of a solid solution between Mn-hydroxides and Fe-hydroxides is feasible. In the Dead Sea, Chain and Discovery Deeps in the Red Sea impurity of Mn in ferrihydrite was observed with an Mn/Fe atomic ratio of 0.013 to 0.244 respectively (Figure 2d).

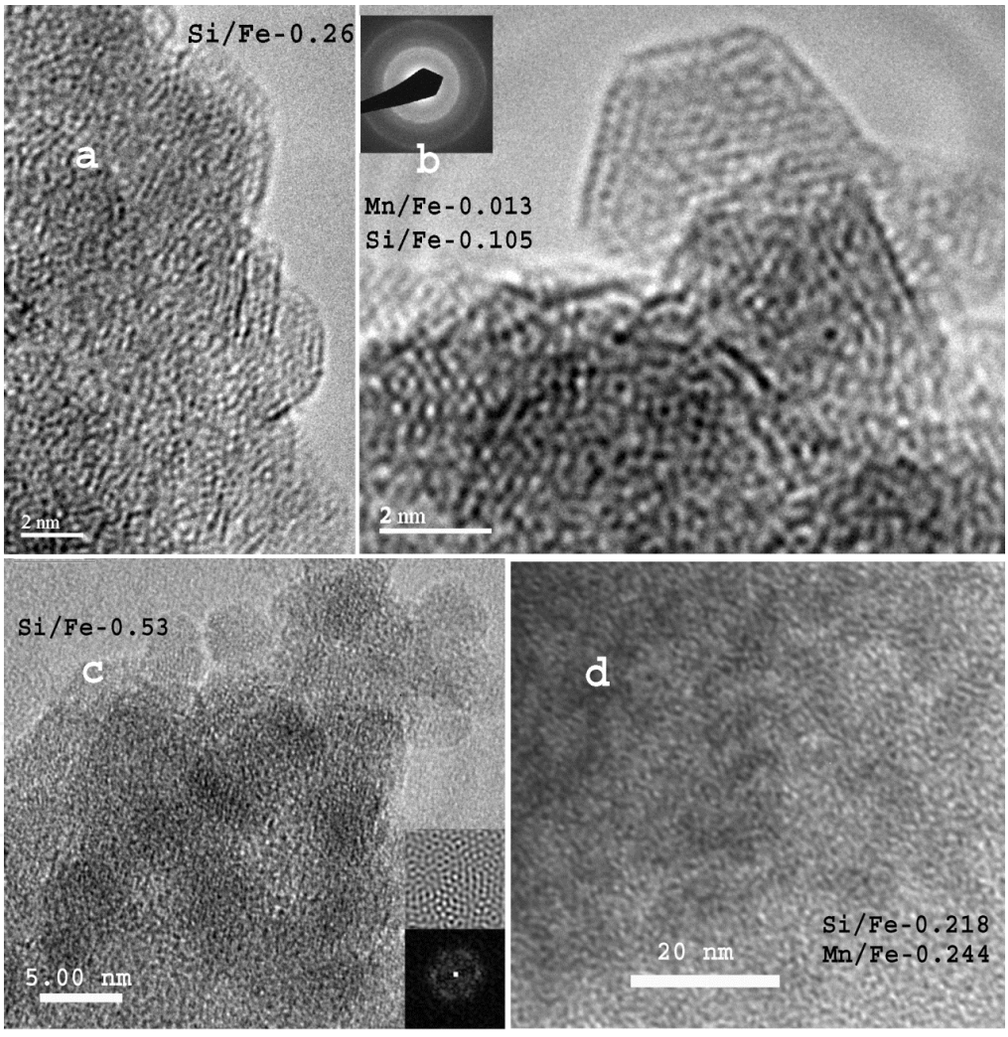

Figure 2. a) 2-line ferrihydrite that crystallized on a floating plastic bag close to a discharging spring into Dead Sea water; b) 2-line ferrihydrite that was preserved within halite crystals. At the upper part of the image, electron diffraction at 0.247 and at 0.1462 nm; c) 2-line ferrihydrite from uppermost centimeter of sediments in the Atlantis II Deep, Red Sea. Electron diffraction yielded 0.25-0.26 and 0.145 nm and Fast Fourier Transformation resulting from the electron diffraction at 0.26 nm; d) ferrihydrite from southern Chain Deep upper 30 cm of the sediments.

3.2. Crystallization of short-range ordered singerite ($SiFe_4O_6(OH)_4*H_2O$)

Singerite appears as rounded platy particles with distinct electron dense, relatively ordered margin and less crystalline inner core. The width of the particles is around 100-200 nm and the dense margins are 5 nm wide [12]. It has a rhombohedral symmetry with unit cell parameters of a=0.504 nm and c=1.08 nm [13]. Singerite was found mainly in the hypersaline hydrothermal brine and the upper sedimental column of the Atlantis II Deep and in the close Chain and Discovery Deeps [14]. Formation in this area results from large amounts of dissolved Si and Fe that lead to formation of short- range ordered phase with elevated atomic Si/Fe ratios (Si/Fe=0.2-0.6). It probably precipitates at the transition zone between the hydrothermal Si-Fe enriched brine and the Red Sea Deep water. Particles of singerite were found in the sediments column down to a depth of few meters with preserved initial morphology.

Synthesis in a brine (40°C, pH7, 2M NaCl) designed to simulate crystallization, singerite was performed successfully with an elevated dissolved initial Si/Fe=1.5 ratio (Figure 3d, e).

3.3. Crystallization of short-range ordered phases Fe-Si-Mn oxides

A short-range ordered Fe-Si-Mn oxide phase made of nano-sized particles forming thin layers that tend to curve and fold was found in the Discovery Deep in the Red Sea. The short-range ordered layers had elevated Si and Mn impurities (Si/Fe of 0.24 and Mn/Fe 0.25) (Figure 3f, g). Association with Si probably hindered crystals growth leading to a short-range ordered phase. The phase resembles in its morphology feroxyhyte but due to elevated Si concentration, it became a short-range ordered phase.

4. Well-crystallized phases

4.1. Crystallization of goethite in the Red Sea Deeps, in the Dead Sea and simulations in vitro

Goethite usually crystallizes from Fe^{2+} at pH 4-9 by fast oxidation/hydrolysis and in the presence of CO_2 [15]. Dissolved Fe^{2+} is supplied by venting hydrothermal hypersaline brines of the Red Sea or in the Dead Sea area. Oxidation of the iron occurred in the Red Sea Deeps as the hydrothermal brine interacts with Red Sea deep water whereas in the Dead Sea area exposure to the atmosphere leads to Fe^{2+} oxidation and goethite precipitation..

Two types of morphologies dominate in most goethite samples of the Red Sea: monodomain, acicular crystals (Figure 4a) and multi-domain crystallites that crystallize from common nuclei and then diverge (Figure 4b, c). Formation of multi-domain crystal of goethite was attributed to the elevated Na concentrations [16] that probably prevail in the hydrothermal brines.

Twinning appears in both morphologies and star-shaped twinning is attributed to formation at elevated temperatures, 60-90°C [17].

Goethite crystals with elevated Si/Fe 0.12 atomic ratios are usually smaller and poorly crystalline, exhibiting numerous crystal defects whereas larger crystals with higher crystal-

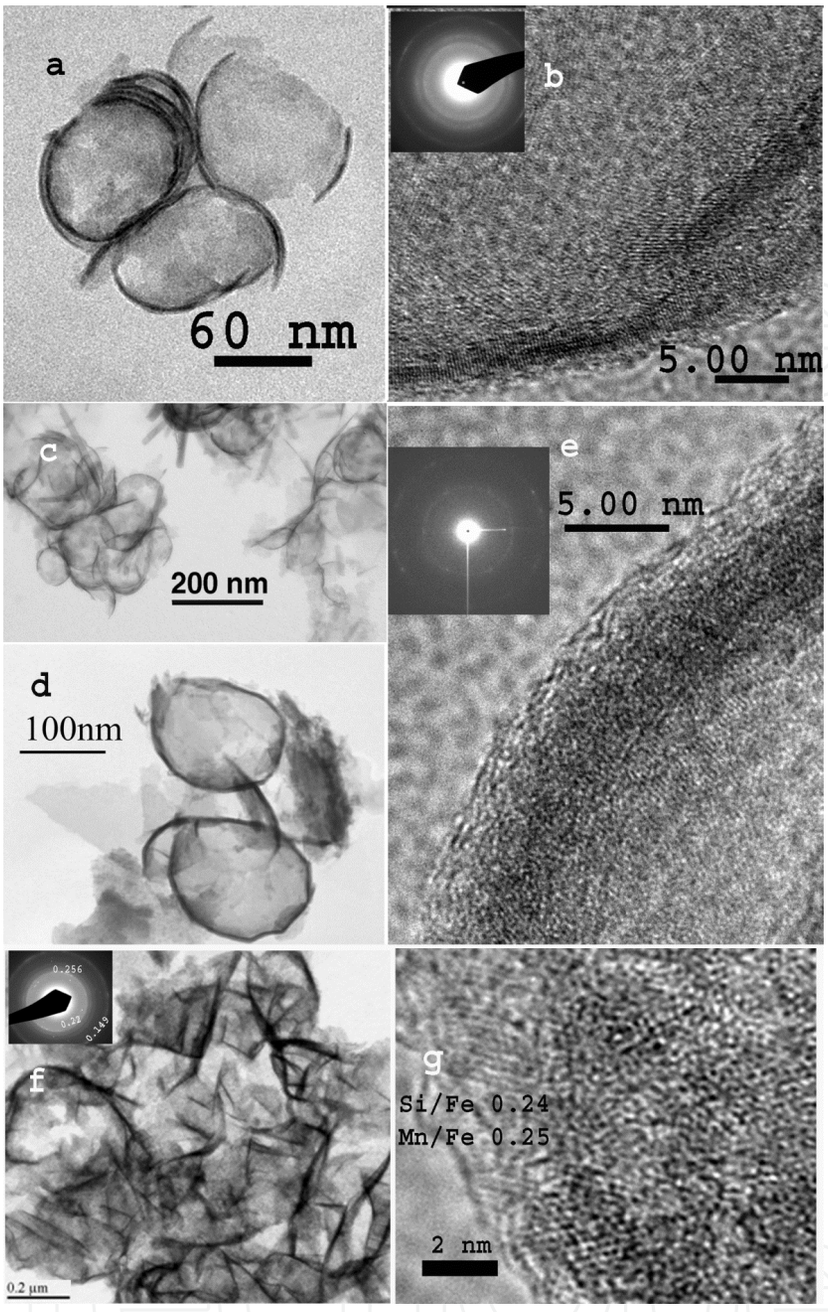

Figure 3. a) Singerite round plates from the Atlantis II Deep, Red Sea; b) High resolution image of the outer rim of the face with short-range ordered inner core. Electron diffraction yielded 0.245 and 0.143 nm; c) Singerite particles from sediments in the Chain Deep; d) Synthetic singerite particles with an outer dense ring; e) High resolution image of synthetic singerite with electron diffraction of 0.25 and 0.27 nm; f) Plates of Fe-Mn-Si oxides from the Discovery Deep; g) High resolution image of the Fe-Si-Mn phase.

linity have a lower Si/Fe elemental ratio. At relatively low Si/Fe ratios, the major effect of Si is to retard growth of the crystallites. Since the amount of soluble Si concentration in the brine was higher in Atlantis II Deep than in Thetis Deep, smaller goethite crystals were formed in the Atlantis II Deep (Figure 4 c, d). Elevated Si concentrations in the brines caused dislocation within the crystals (Figure 4b).

http://dx.doi.org/10.5772/59625

Well-crystallized multi-domain goethite (longer than 500 nm) form mono-layers of iron oxides in the Thetis Deep that were formed at slow oxidation epochs of discharging dissolved Fe^{+2} in a brine with lower Si/Fe values [18].

In the Dead Sea area where Na concentration in the springs or in the brines is high, multi-domain goethite crystallized with a Si/Fe atomic ratio of 0.08 and Mn/Fe 0.04 (Figure 4 e, f)

Star-shaped twinning was observed in a sample from the Atlantis II Deep and in synthesized goethite that crystallized at elevated temperatures (0.8 M NaCl, 60°C) (Figure 4g). At a lower temperature (25°C) synthesized in a 5M NaCl brine, large crystals were formed (Figure 4h) [19].

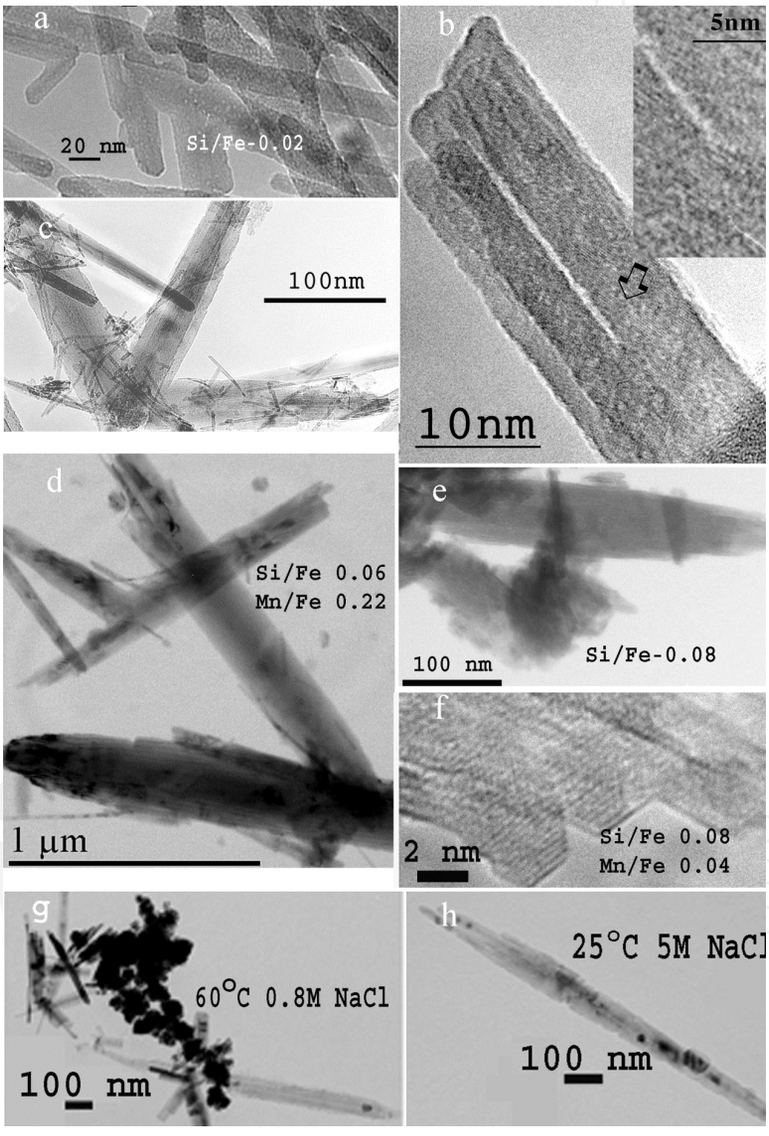

Figure 4. a) Monodomain acicular goethite with twinning from the Atlantis II Deep, Red Sea; b) High resolution image of goethite acicular twins from the Atlantis II Deep, Red Sea; c) Star twinning of multi-domain goethite from Atlantis II Deep, Red Sea; d) Multi-domain goethite from Thetis Deep, Red Sea; e) Multi domain goethite from the Dead Sea area; f) A high resolution image of multi-domain goethite from the Dead Sea; g) Star-shaped multi-domain goethite crystals formed in vitro along with magnetite crystals; h) Multi-domain goethite crystal formed in vitro.

4.2. Crystallization of a solid solution goethite-groutite

Goethite αFeOOH and groutite αMnOOH form a solid solution since both have the structure of Orthorhombic – Dipyramidal H-M Symbol (2/m 2/m 2/m) with space group Pb nm. A solid solution was found in the sediments of the Discovery Deep Mn/Fe 0.33-0.77, Thetis Deep (Mn/Fe 0.10-0.22) in the Red Sea and in sediments that crystallize in the Dead Sea Area (Mn/Fe 0.31) (Figure 5a, b, c).

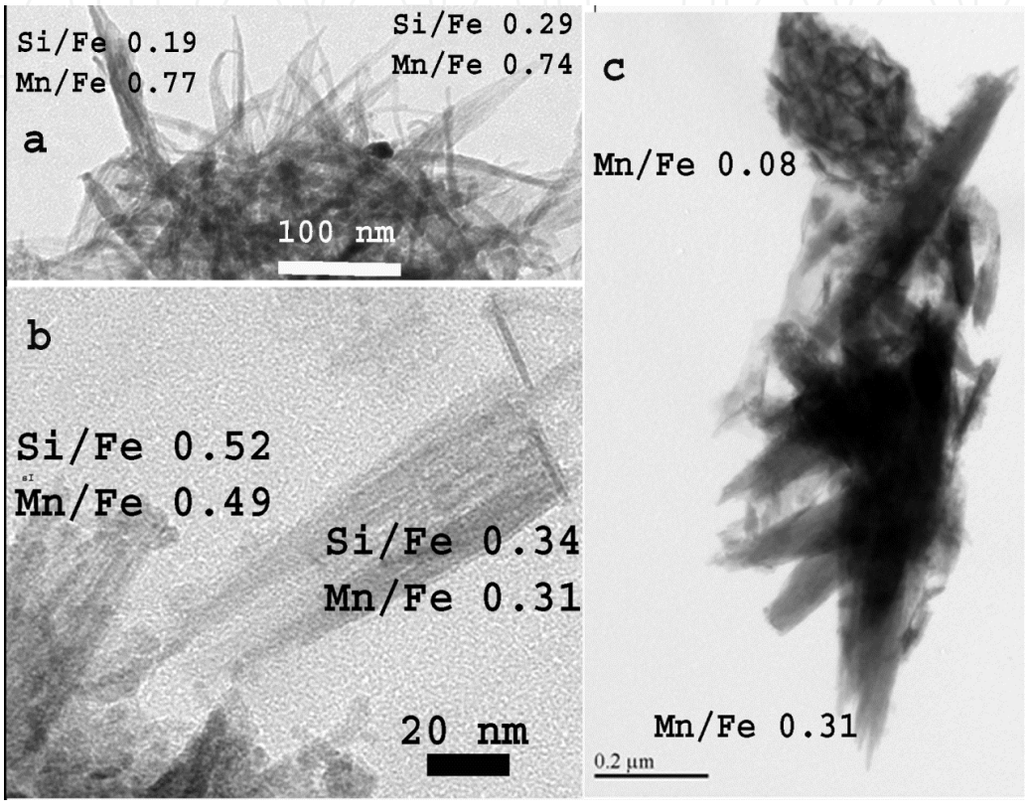

Figure 5. Solid solution of goethite groutite; a, b) Goethite groutite crystals from the Discovery Deep; c) Cluster of goethite-groutite solid solution from the Dead Sea area.

4.3. Crystallization of groutite

Monodomain large crystals of groutite were observed in the southern marginal facies of the Atlantis II Deep of the Red Sea. Impurities of Fe, Si and Ca were found in the crystals. Si retards Mn oxides growth hence lower Si/Mn leads to larger groutite crystals (Figure 6 a, b).

4.4. Crystallization of akaganéite in the Dead Sea area

Akaganeite crystals from the Dead Sea area were crystallized from the hypersaline brine that discharges close to the northern part of the evaporation ponds (Figure 7a). Usually crystallization of akaganéite requires the presence of Cl^- ions for the crystal's stability. In the Dead Sea area, akaganéite were preserved within halite crystals and had acicular or a multi-domain structure (<100 nm) (Figure 7a, b). Incorporation of Si in akaganéite caused twinning [20]

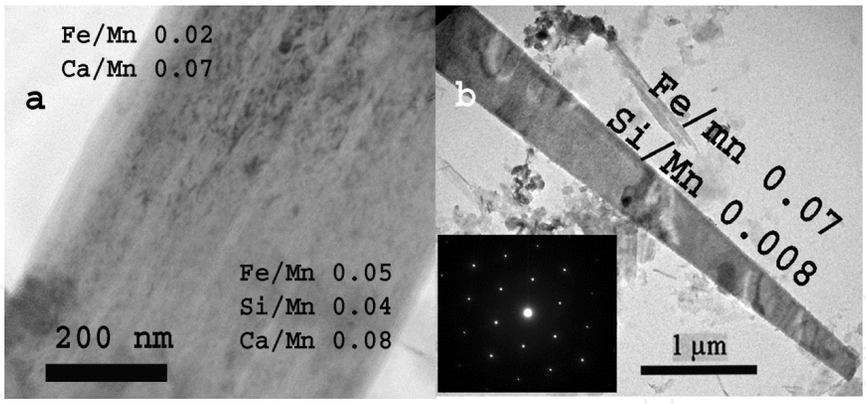

Figure 6. Groutite from the Atlantis II Deep; a) Enlarged image with results of two point analyses; b) Large groutite crystal with electron diffraction.

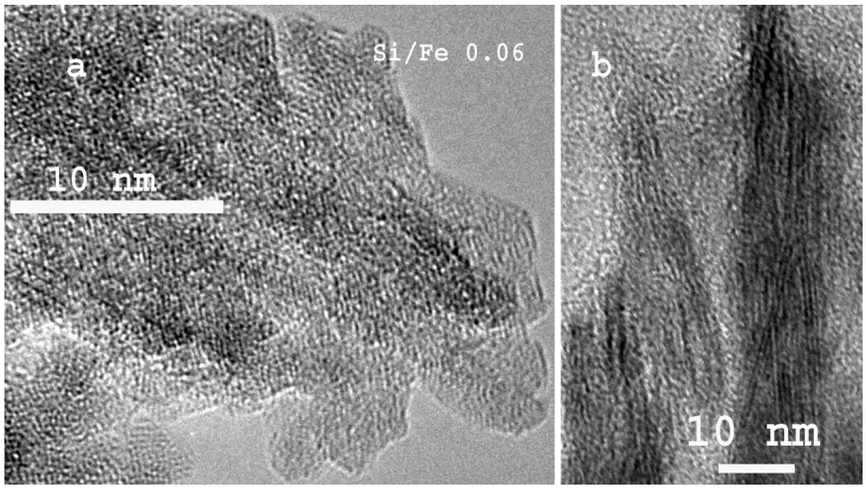

Figure 7. a) Multi-domain akaganéite crystals with Si impurity; b) Acicular crystals of akaganéite with d spacing around 0.7 nm.

4.5. Crystallization of lepidocrocite in the Red Sea Deeps, in the Dead Sea and simulations in vitro

Lepidocrocite usually forms in the presence of chloride at an elevated pH and by slow oxidation relatively to goethite [15]. Three lepidocrocite morphologies were observed in samples from the Atlantis II Deep, Red Sea (Figure 8 a, b): Subhedral plates, rods and multi-domainic crystals, resulting from enhanced crystal growth along the 010 face due to a higher pH [13, 19].

Well-crystallized lepidocrocite of the Thetis Deep in the Red Sea appears as euhedral plates (140-340 nm) or acicular crystals (500-600 nm long and few nm wide) (Figure 8c). In the Discovery Deep, laths-like lepidocrocite were observed (Figure 8d). A high resolution image of platy lepidocrocite from the Thetis Deep had no dislocations and d spacing of 0.62 nm can be observed (Figure 8f).

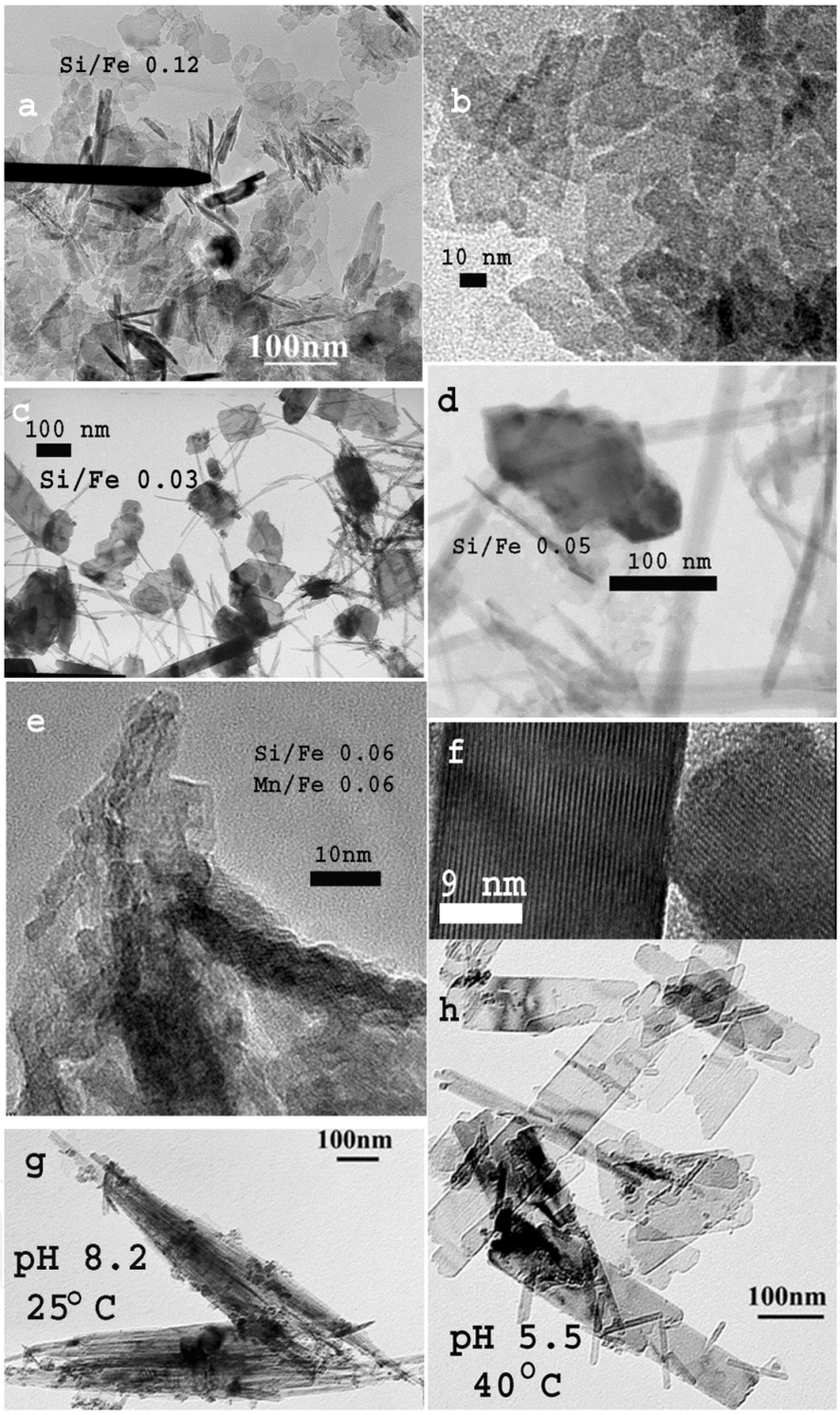

Figure 8. Various morphologies of lepidocrocite: a) Lepidocrocite plates and multi-domain crystals from the Atlantis II Deep, Red Sea; b) Plates of lepidocrocite from the Atlantis II Deep; c) Plates and rods of lepidocrocite from the Thetis Deep, Red Sea; d) Plates of lepidocrocite from Discovery Deep, Red Sea; e) Tiny crystallites of lepidocrocite from the Dead Sea; f) A high resolution image of lepidocrocite crystal from the Thetis Deep Red Sea. (d spacing was 0.62 nm); g) Multi-domain lepidocrocite synthesized at a high pH and low temperature; h) Plates and some rods synthesized at a low pH and elevated temperature.

http://dx.doi.org/10.5772/59625

Platy and rod lepidocrocite from the Thetis and Atlantis II Deeps were probably formed under slightly acidic conditions of the hydrothermal brines. Soluble Si concentration in the brine was higher (Si/Fe 0.11) in the Atlantis II Deep than in the Thetis Deep, leading to larger lepidocrocite crystals in the latter. Lepidocrocite forms mono-layers of iron oxides in Atlantis II and Thetis Deeps due to abrupt oxidation epochs. They were probably formed as down-welling of dense oxidized Red Sea Deep Water formed wide mixing layer which introduced large amounts of dissolved oxygen into the brine leading to abrupt Fe oxidation and lepidocrocite precipitation [21].

Dead Sea lepidocrocite were preserved within halite crystals. In some of the lepidocrocite crystals, impurities of Si and Mn reached the values of Si/Fe 0.06 and Mn/Fe 0.06 (Figure 8e).

Synthesized lepidocrocite morphology changes from plates at pH 5.5 through rods at pH 7 to multi-domainic crystals at pH 8.2, due to enhanced crystal growth along the 010 face (Figure 8g, h). Salinity and temperature have contradictory effects on lepidocrocite crystallinity. Elevated salinity improved lepidocrocite crystallinity while temperature increase had an only partial effect.

4.6. Crystallization of feroxyhyte in the Atlantis II Deep, Red Sea

Feroxyhyte has a morphology of folded layers with Si/Fe=0.3 (Figure 9). Usually feroxyhyte crystallizes over a wide range of pH at high oxidation conditions [15]. Feroxyhyte was found in a sample from the top centimeter of a floppy layer in the Atlantis II Deep [11], indicating that it probably crystallized close to the transition zone between the brine and the Red Sea deep water.

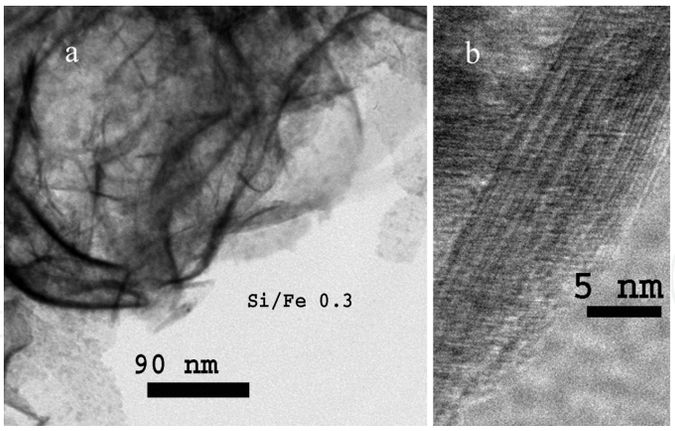

Figure 9. a) Feroxyhyte curved layers from the uppermost layer of sediments in the Atlantis II Deep, Red Sea; b) A high resolution lattice image of feroxyhyte with no dislocations.

4.7. Hematite from the Red Sea

Hematite usually forms by dehydration and rearrangement of ferrihydrite or by thermal transformation from various phases of iron oxides-hydroxides [15]. Hematite usually had platy

morphology (Figure 10a) yet recrystallization of multi-domain iron oxide yielded multi-domain hematite (Si/Fe=0.05) [22].

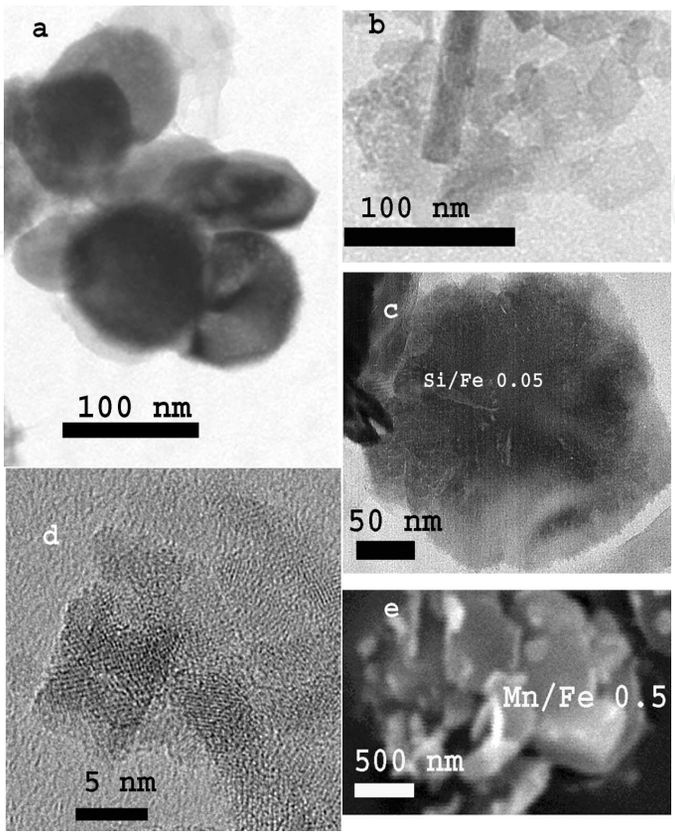

Figure 10. Hematite crystals from the Red Sea Deeps: a) Well-crystallized pure hematite plates from the margins of the Atlantis II Deep; b) Tiny crystallites of hematite from the Discovery Deep and a needle of goethite; c) Large hematite crystal from the lowermost brine in the southwestern part of the Atlantis II Deep; d) A high resolution image of tiny crystallites of hematite from the lowermost brine from the south-western Atlantis II Deep; e) Scanning electron micrograph of hematite plate from the Thetis Deep.

Hematite crystals in the border between the Atlantis II Deep and Chain Deep had a Mn impurity with a Mn/Fe=0.04 ratio. Pure hematite plates were also observed in the Discovery Deep sediments (Figure 10b). Large hematite crystals and nano-sized crystals were found in suspension of the lower hydrothermal brine above the sediments, indicating that they were formed within the brine and not in the sediments (Figure 10c, d).

Hematite crystals from the Thetis Deep had a platy morphology (1-2μm), with an elevated Mn/Fe ratio of 0.5 (Figure 10e). Recrystallization into hematite in the Thetis Deep probably occurred after the hydrothermal discharge ceased and oxygen reached the bottom of the Deep.

4.8. Crystallization of magnetite in the Thetis Deep in the Red Sea and simulations in vitro

Magnetite from the Thetis Deep had octahedral morphology (1-3μm) enriched with small amounts of V, P, and Mn that might have resulted from the leached shales (Figures 11a, b). Similar enrichments in Fe layers were found of the Thetis Deep [23]. It could have precipitated

http://dx.doi.org/10.5772/59625

from a hot (40º-60ºC) and slightly alkaline brine. Incomplete oxidation of dissolved Fe^{2+} led to magnetite crystallization at the lowermost part of the hydrothermal brine. According to the study of rare earth elements, it is possible that hydrothermal saline fluids were temporarily trapped in the Thetis Deep, forming reduced and metal-rich brine bodies [8].

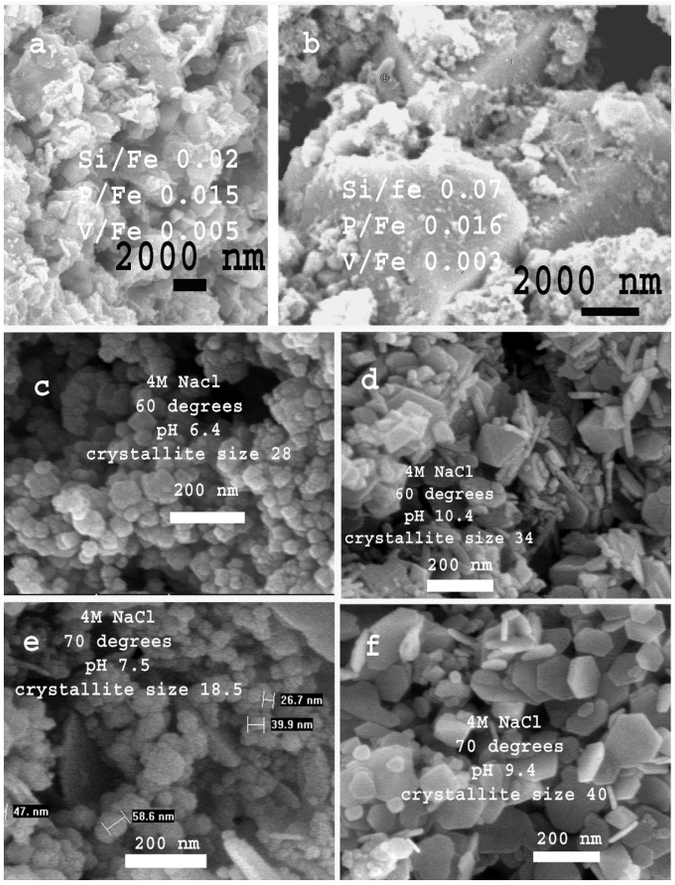

Figure 11. Scanning electron micrographs of magnetite from the Thetis Deep and synthesized in vitro: a) Image of magnetite large crystals from the Thetis Deep partially covered by clay minerals; b) Large crystals of magnetite from the Thetis Deep; c-f) Synthetic magnetite observed by a high resolution scanning electron microscope (HRSEM).

In synthesized magnetite (60°C-80ºC, 0.8, 2, 4, 5 M NaCl and at varying alkalinities pH 6-10.4), crystallite size varied between 18 nm to 45 nm and unit cell parameters varied between 0.8373-0.8396 nm. Morphology varied between euhedral plates or octahedra and unhedral crystals (Figures 11 c-f). The euhedral plates were probably preserving platy green rust or a $Fe(OH)_2$ precursor due to quick crystallization. An increase in pH solution at elevated temperatures (70º and 80ºC) and salinity (4 and 5 M NaCl) yielded magnetite with larger crystallite size and greater unit cell parameters. An opposite trend was observed in magnetite that crystallized at 60ºC, mainly in the 5 M NaCl solution and to a lesser extent in magnetite, crystallized at 4M NaCl solutions.

As observed in previous studies, introducing dissolved silica into the solutions hindered magnetite crystallization and led to decrease in both, crystallite size and unit cell parameters.

4.9. Crystallization of manganite in the Red Sea

Multi-domainic crystals of manganite were observed in sediments from the Chain Deep (200-300 nm), Discovery Deep (>1μm) and from the margins of the Atlantis II Deep. Manganite crystals from the southern Chain Deep had iron impurity Fe/Mn atomic ratios 0.53-0.79 and Si/Mn ratios of 0.14-0.2 (Figure 12a). An elevated Si/Mn ratio probably affected the crystal size of manganite as observed in the crystal size of samples from Chain and Atlantis II Deeps. Manganite crystals from the southern part of the Atlantis II Deep had a Fe/Mn 0.2 ratio and Si/Mn 0.1 ratio (Figure 12c). A high resolution image of manganite crystals from the Atlantis II Deep showed d spacing of 0.48 nm with some dislocations (Figure 12c). Twinning of manganite crystals was observed in the sample from the Discovery Deep (Figure 12d)

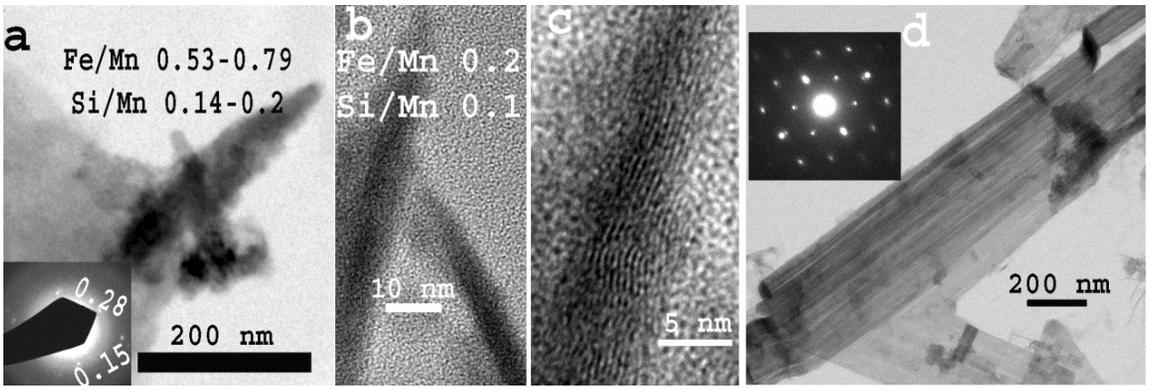

Figure 12. Manganite from the Red Sea: a) Multi-domain manganite from the southern Chain Deep with iron and Si impurities; b) 2 magnetite crystals from the margins of the Atlantis II Deep; c) A high resolution image of manganite from the Atlantis II Deep; d) Twinned manganite crystals from the Discovery Deep with electron diffraction in the upper part.

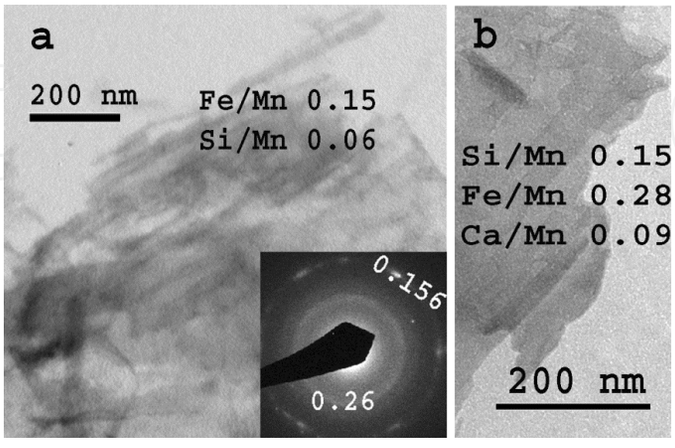

Figure 13. Multi-domain todorokite from the Red Sea Deeps: a) Todorokite from the northern Chain Deep; b) Todorokite from the marginal Atlantis II Deep.

http://dx.doi.org/10.5772/59625

4.10. Crystallization of todorokite in the Red Sea

Plates of todorokite and multi-domain crystals were found in Atlantis II and northern Chain Deeps. Todorokite had Fe and Si impurities with a Fe/Mn atomic ratio of 0.08-0.28 and Si/Mn 0.06-0.15 (Figure 13 a, b). Todorokite crystallized from the hydrothermal brine closer to its origin in the southwestern Atlantis II Deep that overflows into the northern Chain Deep.

5. Conclusions

Crystallization of Fe and Mn oxides - hydroxides occurred in the hypersaline and hydrothermal enviro nment of the Atlantis II, Chain and Discovery Deeps. Iron oxides that were sampled in the Thetis Deep probably crystallized from hydrothermal brine that filled the Deep. Mn oxides - hydroxides were found in the southern part of the Atlantis II and the close Chain and Discovery Deeps in the Red Sea. The minerals studied include short-range ordered ferrihydrite, singerite and Fe-Mn-Si oxides that crystallize at elevated Si concentrations in the brine. Si was found as the main impurity within the phases presented and it hinders crystallization of Fe well-crystallized phases like goethite, lepidocrocite and magnetite or Mn phases like todorokite and manganite. Lower Si concentration in the brine enabled the formation of larger crystals in the Thetis Deep.

Crystallization in hypersaline brine with an elevated Na concentration leads to the formation of multi-domain goethite from the Deeps of the Red Sea and from the Dead Sea. Mn appears as an impurity within iron oxides or forms a solid solution with them. In Mn oxides-hydroxides, Fe appears as an impurity.

Synthesis of the iron oxides hydroxides presented simulated precipitation conditions of the phases.

Author details

Nurit Taitel-Goldman*

Address all correspondence to: nuritg@openu.ac.il

The Open University of Israel, Israel

References

[1] Swift, S.A., Bower, S.A. and Schmidt, R.W., 2012, Vertical, horizontal and temporal changes in temperature in the Atlantis II and Discovery pools, Red Sea. *Deep Sea Research*, 1 64, 118-128.

[2] Schoell, M. and Hartmann, M., 1973, Detailed temperature structure of the hot brines in the Atlantis II Deep area (Red Sea). *Marine geology*, 14, 1-14.

[3] Hartmann, M., 1985, Atlantis II Deep geothermal brine system, Chemical processes between hydrothermal brines and Red Sea deep water. *Marine Geology*, 64, 157-177.

[4] Hartmann, M., Scholten, J.C., Stoffers, P. and Wehner, F.,1998, Hydrographic structure of brine filled deeps in the Red Sea – new results from Shaban, Kerbit, Atlantis II, and Discovery Deep. *Marine Geology*, 144, 311-330.

[5] Shanks, W.C. and Bischoff, J., 1977, Ore transport and deposition in the Red Sea geothermal system: a geochemical model. *Geochimica and Cosmochimica Acta*, 41, 1507-1519.

[6] Laurila, T.E., Hannington, M.D., Petrson, S. and Garbe-Schönberg, 2014, Early depositional history of metalliferous sediments in the Atlantis II Deep of the Red Sea: Evidence from rare earth element geochemistry. *Geochimica et Cosmochimica acta*, 126, 146-168.

[7] Scholten, J.C., Stoffers, P., Walters, P., Pflünger, W., 1991, Evidence for episodic hydrothermal activity in the Red Sea from composition and formation of hydrothermal sediments, Thetis Deep. *Tectonophysics*, 190, 109-117.

[8] Pierret, M.C., Clauer, N. Bosch, D. and Blanc, G., 2010, Formation of Thetis Deep metal rich sediments in the absence of brines, Red Sea, *Journal of Geochemical exploration,* 104, 12-26.

[9] Katz, A., and Starinsky, A., 2009, Geochemical history of the Dead Sea. *Aquat Geochem.* 15, 159-194.

[10] Kawamura, K. and Nissenbaum A., 1992, High abundance of low molecular weight organic acids in hypersaline spring water associated with salt diapir. *Org. Geoche.* 18, 469-476.

[11] Taitel-Goldman, N. and Singer A., 2001, High-resolution transmission electron microscopy study of newly formed sediments in the Atlantis II Deep Red Sea. *Clays and Clay Minerals*, 49, 174-182.

[12] Taitel-Goldman N., Singer A., Stoffers, P., 1999, A new short-range ordered, Fe-Si phases in the Atlantis II Deep, Red Sea hydrothermal sediments. *Proceedings 11th International Clay Conference, Ottawa, Canada 1997 (KodamaH. Mermut A.R. and Torrance J.K. eds.)*, 697-705.

[13] Taitel-Goldman, N. and Singer, A., 2002a, Metastable Si-Fe phases in hydrothermal sediments of Atlantis II Deep, Red Sea. *Clay Minerals*, 37, 236-248.

[14] Taitel-Goldman, N., Ezersky, V. and Mogilianski, D., 2009, High resolution transmission electron microscopy study of Fe-Mn oxides in the hydrothermal sediments of the Red Sea Deeps system. *Clays and Clay Minerals*, 57, 465-475.

[15] Cornell, R.M. and Schwertmann, U., 2003, The Iron Oxides, Structure, Properties, Reactions, Occurrences and Uses. *Wiley-VCH Verlag GmbH & Co. KGaA Weinheim* Pp664.

[16] Cornell, R.M. and Giovanoli, R., 1986, Factors that govern the formation of multi-domain goethites. *Clays and Clay Minerals*, 34, 557-564.

[17] Schwertmann, U., Cambier, P. and Murad, E., 1985, Properties of goethite of varying crystallinity. *Clays and Clay Minerals*, 33, 369-375.

[18] Taitel-Goldman, N., Bender-Koch, C., and Singer, A., 2004, Si associated goethite in hydrothermal sediments of the Atlantis II and Thetis Deeps, Red Sea, *Clays and Clay Minerals*, 52, 115-129.

[19] Taitel-Goldman, N. and Singer, A., 2002b, Synthesis of clay-sized iron oxides under marine hydrothermal conditions. *Clay Minerals*, 37, 719-731.

[20] Cornell, R.M., 1992, Preparation and properties of Si substituted akaganéite (β-FeOOH). *Z. Pflanzenernä*hr. *Bodenk*. 155, 449-453.

[21] Taitel-Goldman, N., Bender-Koch, C., and Singer, A., 2002, lepidocrocite in hydrothermal sediments of the Atlantis II and Thetis Deeps, Red Sea, *Clays and Clay Minerals*, 50, 186-197.

[22] Taitel-Goldman, N., 2009, Nanosized iron oxides and clays of the Red Sea Hydrothermal Deeps. Characterization and formation processes. *VDM Verlg Dr. Müller*, 118Pp

[23] Butuzova, G.Y. and Lyapunov, S.M., 1995, Rare earth elements in hydrothermal sedimentary deposits from the Red Sea. Lithology and Mineral resources, 1, 13-26.

IntechOpen